J Appl Physiol 99: 2045–2052, 2005.
First published July 28, 2005; doi:10.1152/japplphysiol.01138.2004.

HIGHLIGHTED TOPIC | *Biomechanics and Mechanotransduction in Cells and Tissues*

Biomechanical and phenotypic changes in the vasospastic canine basilar artery after subarachnoid hemorrhage

Mitsuo Yamaguchi-Okada, Shigeru Nishizawa, Masayo Koide, and Yuichiro Nonaka

Department of Neurosurgery, Hamamatsu University School of Medicine, Hamamatsu, Shizuoka, Japan

Submitted 14 October 2004; accepted in final form 22 July 2005

Yamaguchi-Okada, Mitsuo, Shigeru Nishizawa, Masayo Koide, and Yuichiro Nonaka. Biomechanical and phenotypic changes in the vasospastic canine basilar artery after subarachnoid hemorrhage. *J Appl Physiol* 99: 2045–2052, 2005. First published July 28, 2005; doi:10.1152/japplphysiol.01138.2004.—Because it has been argued that active myogenic tone prolongs cerebral vasospasm for >2 wk after subarachnoid hemorrhage (SAH), we attempted to identify the mechanism that plays the main role in sustaining the prolonged cerebral vasospasm. We especially focused on the roles of biomechanical and phenotypic changes in the cerebral arteries in the mechanisms of prolonged vasospasm after SAH. We used the basilar arteries from a "two-hemorrhage" canine model to make serial measurements of maximal contraction capacity and arterial stiffness (papaverine-insensitive tone) until *day 28*. We also examined hematoxylin-eosin-stained vasospastic canine basilar arteries for histological changes and immunohistochemically examined them for expression of myosin heavy chain isoforms (SMemb, SM1, and SM2), which are markers of smooth muscle phenotypic changes. Changes in collagen concentration in canine basilar arteries were also measured. Angiographic cerebral vasospasm persisted until *day 14* and then gradually diminished; artery diameter returned to the control diameters on *day 28*. Maximal contraction capacity decreased until *day 21* and showed some recovery by *day 28*. Arterial stiffness, on the other hand, progressed until *day 28*. Histological examination revealed medial thickening and increased connective tissue until *day 21* and a return to control findings by *day 28*. The increased connective tissue was not accompanied by changes in collagen concentration, suggesting a role of some other protein in the increase in connective tissue. Immunohistochemical studies with anti-SMemb, anti-SM1, and anti-SM2 antibodies showed enhanced expression of SMemb from *day 7* to *day 21* and disappearance of SM1 and SM2 on *days 14* and *21*. The changes in myosin heavy chain isoform expression returned to normal on *day 28*. The above results indicate that biomechanical and phenotypic changes may play a pivotal role in sustaining cerebral vasospasm for >2 wk after SAH, with minimal changes in active myogenic arterial tone.

biomechanics; cerebral vasospasm; vascular smooth muscle

CEREBRAL VASOSPASM AFTER subarachnoid hemorrhage (SAH) is a characteristic phenomenon that is observed in the cerebral arteries alone. When SAH occurs, the cerebral arteries strongly contract for more than 2 wk. Vascular smooth muscle contraction is known to be caused by interaction between actin and myosin in vascular smooth muscle cells, but it has not been clarified whether sustained active myogenic tone is the sole mechanism responsible for the prolonged cerebral vasospasm after SAH, or whether there are other mechanisms that contribute to it (3, 4, 6, 10, 11, 13, 14, 17, 18, 22, 25, 26, 28, 30, 32, 33, 36). In our previous reports of studies of intracellular signal transduction in a "two-hemorrhage" canine model (34), we found that PKC plays a pivotal role in cerebral vasospasm until *day 7* (22, 25, 26), and we found a more important role for protein tyrosine kinase in the later stage in the 2-wk model (14). We also showed that in situ treatment with PKC inhibitors significantly inhibits cerebral vasospasm despite augmented myosin light chain phosphorylation levels (26). There have also been conflicting reports that active myogenic contraction of cerebral arteries is attenuated (13) or enhanced by nonmuscle arterial constriction during cerebral vasospasm (10). Histological changes, such as degeneration (6), fibrosis (6, 10), myonecrosis (11), or vascular cell proliferation (4, 6), are known to occur in the vascular wall of vasospastic arteries, raising the possibility that the persistence of cerebral vasospasm after SAH, especially during the late phase, might not be induced by simple active myogenic tone of vascular smooth muscle cells.

Vascular smooth muscle undergoes phenotypic changes with the cell cycle and in response to physical and/or chemical stimulation (1, 7, 8, 15, 16, 19, 20, 27, 29). There are two types of vascular smooth muscle cells, a synthetic (or embryonal) type and a contractile (or adult) type (27, 29, 31). Vascular smooth muscle cells of synthetic (or embryonal) type are observed in the arterial wall of an embryo and in cultured cells and contribute to protein synthesis and production of extracellular matrix. On the other hand, vascular smooth muscle cells of contractile (or adult) type are observed in the medial layer of adult arterial smooth muscle cells and contain abundant muscle filament. Vascular smooth muscle changes from the synthetic type to the contractile type during the process of maturation (differentiation), and the opposite occurs in some pathological processes, such as arteriosclerosis or restenosis of coronary arteries after balloon angioplasty or insertion of an arterial stent (dedifferentiation) (29). These changes are defined as "phenotypic changes."

All these reports describing phenotypic changes of vascular smooth muscle cells suggest that some other mechanisms, such as biomechanical and phenotypic changes, sustain cerebral vasospasm in the late phase after SAH instead of active myogenic vascular tone alone. Most previous studies using animal models to investigate the mechanism of cerebral vasospasm after SAH have investigated the acute phase (within 1

Address for reprint requests and other correspondence: S. Nishizawa, Dept. of Neurosurgery, Hamamatsu Univ. School of Medicine, 1-20-1 Handayama, Hamamatsu, Shizuoka, 431-3192 Japan (e-mail: nisizawa@hama-med.ac.jp).

The costs of publication of this article were defrayed in part by the payment of page charges. The article must therefore be hereby marked "*advertisement*" in accordance with 18 U.S.C. Section 1734 solely to indicate this fact.

wk). However, because human cerebral vasospasm persists for over 2 wk, it is important to examine vasospastic cerebral arteries for more than 1 wk. It thus might appear that the properties of cerebral vasospastic arteries after SAH show significant changes in mechanisms required to sustain vasospasm over prolonged periods (14).

In this study, we investigated the role of biomechanical and phenotypic changes in vasospastic cerebral arteries, in a 1-mo animal model of SAH to identify the mechanism that plays the main role in sustaining the prolonged vasospasm. We measured maximal contractility, and active myogenic and nonmyogenic tone in long-lasting cerebral vasospastic arteries in an isometric tension study, examined the arteries for histological changes, stained them immunohistochemically, and measured the collagen concentrations in the arteries.

MATERIALS AND METHODS

Animals

All experiments were performed according to the Rules of Animal Experimentation and the Guide for the Care and Use of Laboratory Animals of Hamamatsu University School of Medicine.

Animal Model of Cerebral Vasospasm

An experimental animal model of SAH and cerebral vasospasm was produced by modifying the two-hemorrhage canine model (25, 26) originally described by Varsos et al. (34). Beagle dogs of either sex weighing 7–10 kg were anesthetized by intravenous injection of pentobarbital sodium (25 mg/kg), and a tracheal tube was inserted. A sterile catheter was inserted into the vertebral artery on each side under fluoroscopic control via the femoral artery, and the head of the dog was fixed in a stereotactic frame. A control angiogram of the canine basilar artery was obtained by injecting 7 ml of Iopamirone 300 (Schering, Osaka, Japan). End-tidal CO_2 was maintained at 38–42 Torr throughout the angiography. After the control angiogram was obtained, 3 ml of autologous arterial blood were manually injected into the cisterna magna (*day 1*), and the same amount of autologous arterial blood was injected into the cisterna magna on *day 4*. Dogs were randomly divided into four groups, and the final angiography was taken on *days 7*, *14*, *21*, and *28*, respectively. After the final angiography, the dogs were killed by bolus injection of an excess dose of pentobarbital sodium (50 mg/kg), and the basilar artery was quickly excised with the brain stem. The basilar artery was immersed in the dissecting buffer solution (in mM: Na^+ 144.44; K^+ 4.10; Cl^- 135.02; Ca^{2+} 1.01; Mg^{2+} 1.19; PO_4^{3-} 1.54; SO_4^{2-} 1.19; *N*-2-hydroxyethylpiperadine-*N*′-2-ethanesulfonic acid 24.90; glucose 10.0) as described previously (23). The solution was aerated with 100% O_2, and the pH and temperature were adjusted to 7.40 and 37.0 ± 0.2°C, respectively. The excised basilar artery was dissected from the brain stem and the arachnoid membrane under a microscope. Clotted blood around the artery was meticulously removed under the microscope, and intraluminal blood was flushed out with dissecting buffer before the basilar artery was used in the experiments. Control experiments in the isometric tension study were performed by using canine basilar arteries on which angiography was performed without blood injection.

The angiographic diameter of the basilar artery on the angiogram was measured by dividing the artery into three segments and measuring the diameter of each segment at its midpoint under a microscope. The diameter of the arteries is expressed as the mean ± SE of the values in the three segments, and the diameter on *days 7*, *14*, *21*, and *28* is expressed as a percentage of the diameter on *day 1* (=100%).

Isometric Tension Study

An isometric tension study was performed on isolated canine basilar arteries, with a self-designed apparatus as previously described (23). Three arterial rings were obtained from each basilar artery by cutting it into 4-mm length. Each arterial ring was used for a different study. The endothelium of each arterial ring was gently rubbed with a stainless steel wire as described previously (21). After insertion of two wires in the lumen of the arterial ring and setting in the chamber of the apparatus, an arterial ring was perfused in the chamber with physiological saline solution (PSS; in mM: Na^+ 144.44; K^+ 4.10; Cl^- 127.2; Ca^{2+} 2.49; Mg^{2+} 1.19; PO_4^{3-} 1.54; SO_4^{2-} 1.12; HCO_3^- 24.9; glucose 5.0) aerated with 20% O_2, 5% CO_2, and 75% N_2. The pH of the solution and the temperature in the chamber were adjusted to pH 7.40 ± 0.02 and 37.0 ± 0.2°C.

After incubating the arterial ring with PSS in the chamber without stretching for 20 min, the arterial ring was stretched in a stepwise fashion. First, tension that developed in the high-K^+ solution (in mM: Na^+ 72.2; K^+ 76.3; Cl^- 127.2; Ca^{2+} 2.49; Mg^{2+} 1.19; PO_4^{3-} 1.54; SO_4^{2-} 1.12; HCO_3^- 24.9; glucose 5.0) was measured in arterial rings obtained on each day (*days 1*, *7*, *14*, *21*, and *28*) to induce the maximal active myogenic tone.

By use of another arterial ring, the stiffness of arterial wall was examined. An arterial ring was stretched by separating the two wires in a stepwise fashion to the same circumference as obtained in situ by angiography. The distance between the two wires stretching the arterial ring was computed as follows: $d = \pi (R - r)/2$ (d, distance between the wires; π, ratio of the circumference of a circle to its diameter; R, diameter of the basilar artery on the angiogram, r, diameter of the wire = 0.16 mm) (24). After separating the wires to stretch the arterial ring, the tension that developed reached a plateau, and papaverine (from 10^{-6} to 10^{-3} M) was applied. Because the maximal relaxation was obtained at the concentration of 10^{-4} M and the magnitudes of relaxation between at 10^{-4} and 10^{-3} M were not statistically different (data not shown), the concentration of papaverine at 10^{-4} M was used in the subsequent experiments. The tension that developed was composed of two components, a papaverine-sensitive component and a papaverine-insensitive component. The total amount of tension that developed and papaverine-sensitive tone and papaverine-insensitive tone were measured and compared. Papaverine-sensitive and -insensitive tones are expressed as percentages of the total developed tension when the wires were separated according to the formula described above.

Because the amount of tension that developed in the isometric tension study depended on the length of the arterial ring, the length of the arterial rings was carefully measured with a vernier micrometer at the end of experiments, and any tension that developed in this study was expressed in units of grams per millimeter artery length (g/mm).

Histological Examination

Twenty dogs were used for histological examination. The dogs were randomly divided into five groups ($n = 4$ each): a control group and SAH groups killed on *days 7*, *14*, *21*, and *28*. In the dogs belonging to the control group, angiography was not performed. All dogs were killed as described earlier. To fix the basilar arteries, thoracotomy was performed, and after ligation of the descending aorta, a 4.0% paraformaldehyde was perfused through a catheter inserted in the left ventricle of the heart and was drained from the right atrium. Basilar arteries were removed and stored in paraformaldehyde at 4°C. For histological examination, the basilar arteries were embedded in paraffin and cut into 4-μm sections. After hematoxylin-eosin staining and Azan staining, the basilar arteries were examined under a light microscope.

To investigate vasospastic canine basilar arteries for phenotypic changes, arteries were immunohistochemically stained for expression of myosin heavy chain (MHC) subtypes with a monoclonal antibody against embryonal nonmuscle MHC (SMemb; 1:3,000) and antibodies

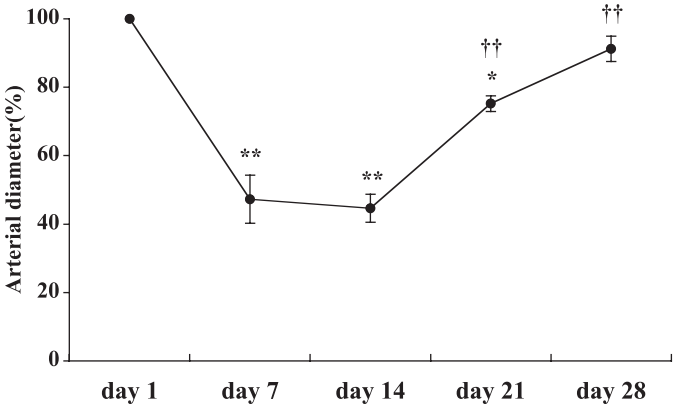

Fig. 1. Changes in the angiographic diameter of the canine basilar artery in a "2-hemorrhage" canine model. Arterial diameter on *days 7*, *14*, *21*, and *28* is expressed as a percentage of the control diameter, and the data are reported as means ± SE. *$P < 0.05$ vs. *day 28*. **$P < 0.01$ vs. *day 28*. ††$P < 0.01$ vs. *days 7* and *14*.

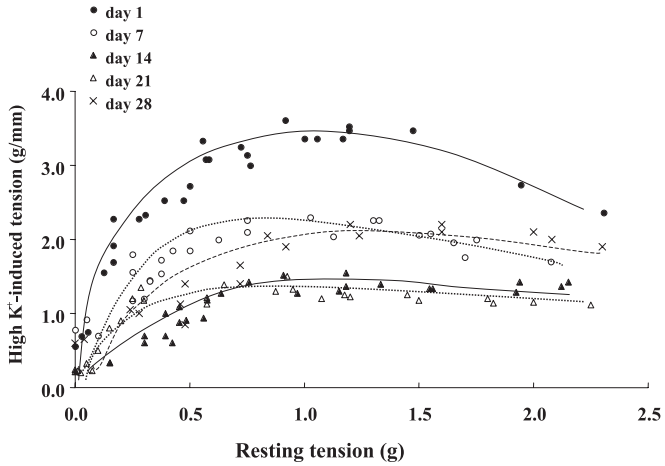

Fig. 2. Tension developed in response to high-K^+ solution in an arterial ring obtained on different days after subarachnoid hemorrhage at different resting tensions. All arterial rings developed maximal tension at a resting tension of 1.0 g. The tensions that developed are expressed as g/mm length of the arterial ring (g/mm).

against the contractile types of smooth muscle MHC (SM1; 1:3,000 and SM2; 1:400). The sections were counterstained with hematoxylin, and the sections were examined for immunoreactivity with each antibody under a light microscope. By use of an image analysis software (NIH Image), immunoreactivity was quantitatively analyzed by setting a 50 × 50 μm square over the most intensely stained area and performing densitometric scans. The results are expressed in arbitrary densitometric units.

Collagen Measurement

Another 20 dogs were prepared to measure the collagen concentration in the basilar artery and were divided into five groups ($n = 4$ each): a control group and groups killed on *days 7*, *14*, *21*, and *28*. In the dogs belonging to the control group, angiography was not performed. Arteries were excised quickly, frozen in liquid nitrogen, and stored at −80°C. A Sircol collagen assay kit (Biocolor, Belfast, UK) that uses a quantitative dye-binding method was designed for in vitro analysis of collagen in biological material. Three sets of 1.5-ml microcentrifuge tubes were prepared: reagent blanks (100 μl of 0.5 M acetic acid), collagen standards (12.50, 25.00, and 50.00 μg), and basilar artery samples (weight: 0.50–0.90 mg). Arterial tissue was minced and homogenized in 100 μl of extraction buffer (in M: Na^+ 2.0; Cl^- 2.0; acetic acid 0.5) to extract salt- and acid-soluble collagen. After centrifugation at 15,000 *g* for 5 min, the supernatants containing soluble collagen were collected. After addition of 100 μl of distilled water to each pellet, which contained insoluble collagen, samples were incubated at 80°C for 60 min to denature the insoluble collagen. Equal volumes of the supernatant containing salt- and acid-soluble collagen and the solution containing denatured insoluble collagen were mixed together and adjusted to 100 μl with 0.5 M acetic acid. After addition of 1 ml of Sircol dye reagent to each tube, the tubes were placed in a shaker and shaken gently for 30 min. The collagen-dye complex precipitated during the mixing, and the tubes were then centrifuged at 15,000 *g* for 15 min. The supernatant, which was dye-unbound solution, was discarded, and 1 ml of the alkali reagent was added to the pellet to dissolve the collagen-dye complex. A 100-μl aliquot of each sample was placed in the wells of a microwell plate, and the absorbance of the reagent blanks, multiconcentrated collagen standards, and test samples was measured at 540-nm wavelength with a spectrophotometer. A standard curve was plotted from the collagen standard, and the collagen content of each sample was determined from the standard curve. Collagen concentrations are expressed as micrograms per milligram weight of the basilar artery.

Drugs

Iopamirone 300 was purchased from Japan Schering (Osaka, Japan). Pentobarbital sodium was obtained from Dinabot (Osaka, Japan). Papaverine was purchased from Sigma Chemical (St. Louis, MO). The other agents were obtained from Wako Pure Chemical Industries (Osaka, Japan). A stock solution of papaverine at a concentration of 10^{-1} M was prepared in PSS and stored at −80°C. Anti-SMemb, anti-SM1, and anti-SM2 mouse monoclonal antibodies were purchased from Yamasa, Chiba, Japan.

Statistical Analysis

All data are expressed as means ± SE. Paired or unpaired Student's *t*-tests were used to examine pairs of groups for statistically significant differences. Differences among groups were analyzed for statistical significance by Dunnett's multiple comparison tests after ANOVA. A *P* value of <0.05 was considered statistically significant.

RESULTS

Angiographic Diameter of the Basilar Artery

The angiographic diameter of canine basilar arteries was 1.41 ± 0.05 mm on *day 1* (control = 100%, number of dogs;

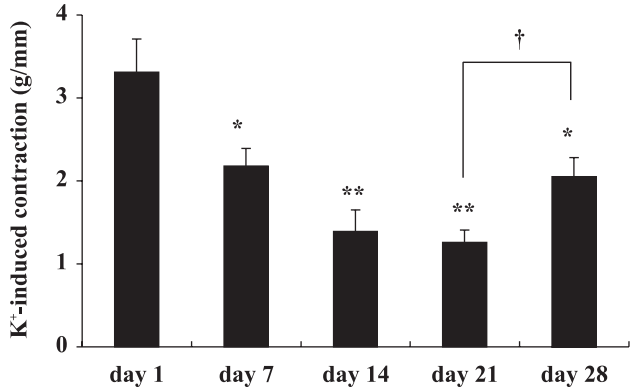

Fig. 3. Maximal tension (g/mm) developed in the canine basilar artery in response to high-K^+ solution in the isometric tension study. Basilar arteries were obtained from control dogs and dogs killed on *days 7*, *14*, *21*, and *28* in the 2-hemorrhage canine model. *$P < 0.05$ vs. *day 1*. **$P < 0.01$ vs. *day 1*. †$P < 0.05$ between the values on *days 21* and *28*.

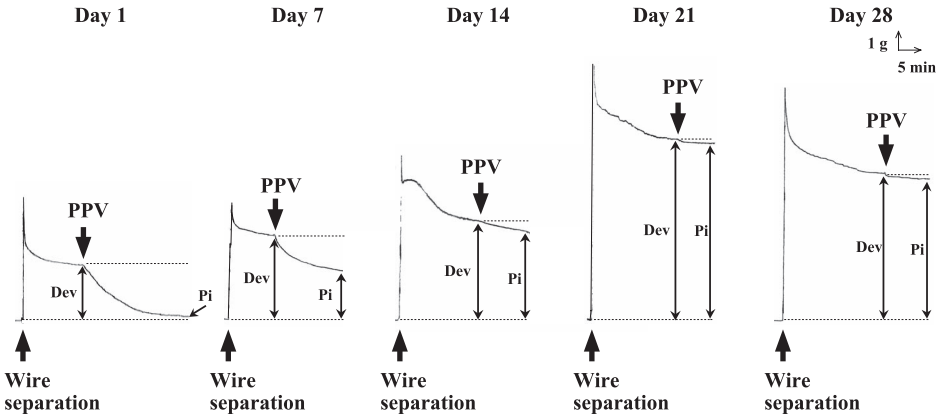

Fig. 4. Representative traces in the isometric tension study showing total developed tension, papaverine-sensitive tension, and papaverine-insensitive tension of an arterial ring obtained on each day. Dev, total developed tension by wire separation; PPV, papaverine; Pi, papaverine-insensitive tone.

$n = 5$). The diameter of the basilar arteries on *days 7*, *14*, *21*, and *28* was 47.3 ± 7.0% ($n = 5$), 44.6 ± 4.1% ($n = 5$), 75.2 ± 2.3% ($n = 5$), and 91.2 ± 3.7% ($n = 5$), respectively. The difference in arterial diameter between *days 7* and *14* was not statistically significant. After *day 14*, the angiographic cerebral vasospasm gradually attenuated, and arterial diameter on *days 21* and *28* was significantly different from the diameter on *days 7* and *14* ($P < 0.01$). The arterial diameter on *day 28* was almost the same as the control diameter on *day 28* (Fig. 1).

Isometric Tension Study

High-K^+-induced vasocontraction. At first, the optimal resting tension for arterial rings obtained on different days after SAH to induce the maximal tension developed in response to high-K^+ solution was examined. Because the maximal tension that developed in the high-K^+ solution occurred at a resting tension of 1.0 g, the resting tension in the subsequent experiments was set at 1.0 g (Fig. 2). The maximal contraction of the arterial rings induced by high-K^+ solution was 3.31 ± 0.40 g/mm on *day 1*, 2.18 ± 0.21 g/mm on *day 7*, 1.39 ± 0.26 g/mm on *day 14*, 1.26 ± 0.15 g/mm on *day 21*, and 2.05 ± 0.23 g/mm on *day 28* ($n = 5$ arterial rings in each group). The maximal contraction elicited by high-K^+ solution on *days 7* ($P < 0.05$), *14* ($P < 0.01$), *21* ($P < 0.01$), and *28* ($P < 0.01$) was significantly lower than the control arteries on *day 1* (Fig. 3). The greatest decrease in contractility was observed in the artery on *day 21*, and contractility gradually increased in the artery on *day 28*. Contractility on *day 28* was statistically different from that on *day 21* ($P < 0.05$).

Papaverine-sensitive and -insensitive tones. Arterial rings were stretched to the same circumference as in the angiogram, as calculated by the formula described in MATERIALS AND METHODS, and total tension that developed was measured. Papaverine (10^{-4} M) was then applied to the tissue to eliminate papaverine-sensitive tone. Total developed tension was 0.7 ± 0.07 g/mm on *day 1*, 1.1 ± 0.10 g/mm on *day 7*, 1.3 ± 0.15 g/mm on *day 14*, 2.8 ± 0.35 g/mm on *day 21*, and 2.1 ± 0.24 g/mm on *day 28* ($n = 5$ arterial rings in each group). Total developed tension on *days 7* ($P < 0.05$), *14* ($P < 0.05$), *21* ($P < 0.01$), and *28* ($P < 0.05$) was significantly greater than on *day 1*. Papaverine-insensitive tone, i.e., the tension remaining after applying papaverine, was 1.5 ± 3.2% on *day 1*, 52.7 ± 5.4% on *day 7*, 94.6 ± 2.9% on *day 14*, 90.9 ± 8.5% on *day 21*, and 91.7 ± 4.3% on *day 28* ($n = 5$ arterial rings in each group). The level of papaverine-insensitive tone on *days 7*, *14*, *21*, and *28* was significantly greater than that on *day 1* ($P < 0.01$), and the level on *days 14*, *21*, and *28* was also was significantly greater than on *day 7* ($P < 0.01$). The differences between papaverine-insensitive tone on *days 14*, *21*, and *28* were not statistically significant. Representative traces from the isometric tension study showing total developed tension, papaverine-sensitive tension, and papaverine-insensitive tension on each day are shown in Fig. 4, and the data are summarized in Fig. 5.

Histological Examination

Hematoxylin-eosin staining and Azan staining. Hematoxylin-eosin-stained smooth muscle cells of the control artery exhibited spindle-like morphology (Fig. 6, *top*). Histological examination of the basilar arteries collected on *days 7*, *14*, and *21* after SAH showed that the smooth muscle cells became shorter and rounder with time, and thickening of the smooth muscle layer was also

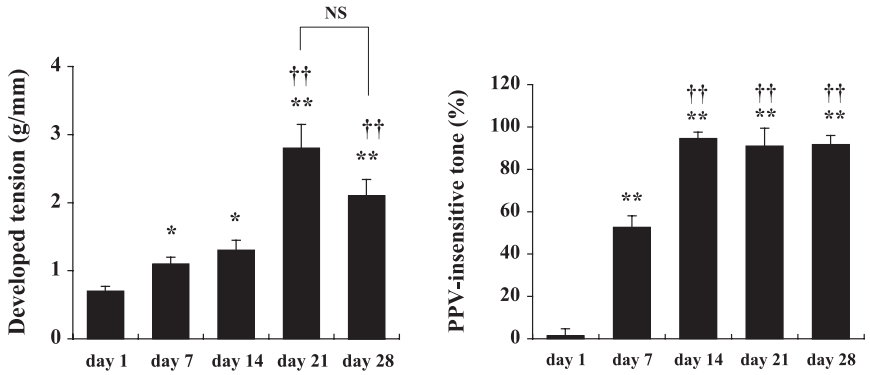

Fig. 5. Total developed tension produced by stretching the arterial rings by separating the 2 wires (*left*), and papaverine-insensitive, nonmyogenic tone (*right*) in each canine basilar artery. Total developed tension is expressed as g/mm, and the data are expressed as a percentage of total developed tension and reported as means ± SE. *$P < 0.05$ vs. *day 1*. **$P < 0.01$ vs. *day 1*. ††$P < 0.01$ vs. *day 7*. NS, not significant.

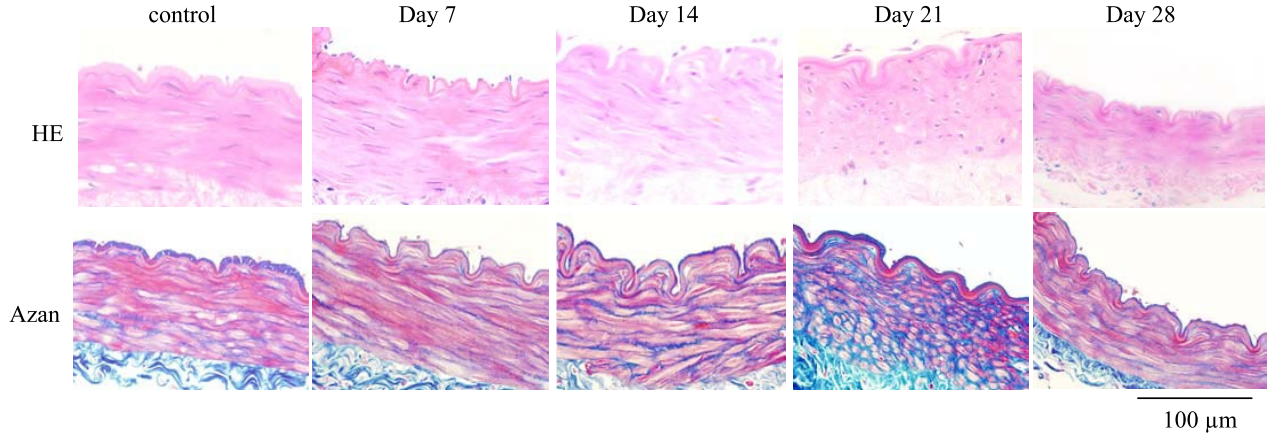

Fig. 6. Histological findings of canine basilar arteries on each day, stained with hematoxylin-eosin (HE; *top*) and Azan stain (*bottom*).

detected on *days 14* and *21*. The most significant histological changes in the canine basilar artery were observed on *day 21*. Endothelial detachment was observed on *days 7*, *14*, and *21*. The changes in the endothelial lining and the thickening of the medial layer were less marked by *day 28*, but the smooth muscle cells were still short and rounded. The connective tissue in the control artery was stained partly in the medial muscle layer and mostly in the adventitial layer with Azan stain (Fig. 6, *bottom*). On the other hand, increased staining of connective tissues was observed, especially in the medial layer in the arteries on *days 7*, *14*, and *21* compared with the control artery. These changes were progressive, and the most significant changes in Azan staining were observed on *day 21*. These changes in the medial layer were no longer seen by *day 28* after SAH, and the Azan staining on *day 28* had returned to the control level (Fig. 6, *bottom*).

Expression of MHC subtypes. Representative immunohistochemical findings with anti-SMemb, anti-SM1, and anti-SM2 antibodies are shown in Fig. 7. The results of the densitometric analysis of SMemb immunoreactivity in the control and vasospastic arteries on each day were 2,346 ± 389 in the control, 12,149 ± 1,108 on *day 7*, 13,826 ± 1,268 on *day 14*, 9,519 ± 792 on *day 21*, and 4,597 ± 563 on *day 28* ($n = 4$ each). The results for SM1 in the control and on *days 7*, *14*, *21*, and *28* were 13,293 ± 987, 14,322 ± 1,312, 4,064 ± 561, 2,417 ± 350, and 12,642 ± 1,056, respectively. The results for SM2 in the control and on *days 7*, *14*, *21*, and *28* were 12,645 ± 1,021, 11,800 ± 1,266, 3,568 ± 489, 1,359 ± 211, and 10,712 ± 984, respectively. These data and the results of the statistical analysis are summarized in Fig. 8. SMemb immunoreactivity on *days 7* ($P < 0.01$), *14* ($P < 0.01$), and *21* ($P < 0.01$) was significantly higher than in the control but had decreased by *day 28*. SM1 and SM2 immunoreactivity, on the other hand, was significantly decreased on *days 14* and *21* compared with the control ($P < 0.01$ each) but returned to the control level by *day 28*.

Collagen Concentration in Basilar Arteries

The collagen concentration was 304.3 ± 33.0 μg/mg ($n = 4$) in the control artery, and on *days 7*, *14*, *21*, and *28* after SAH, it was 341.9 ± 77.0 ($n = 4$), 436 ± 31.1 ($n = 4$),

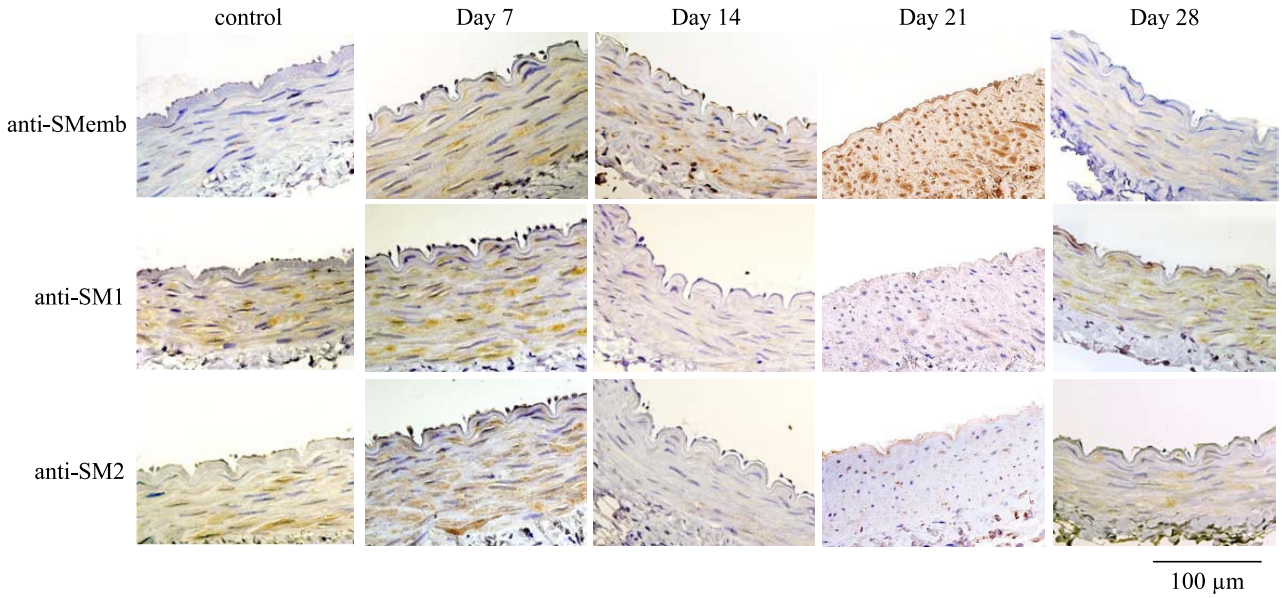

Fig. 7. Immunohistochemical staining of canine basilar arteries on each day with monoclonal antibodies to myosin heavy chain (MHC) isoforms. SMemb, embryonal nonmuscle MHC; SM1 and SM2, contractile types of smooth muscle MHC.

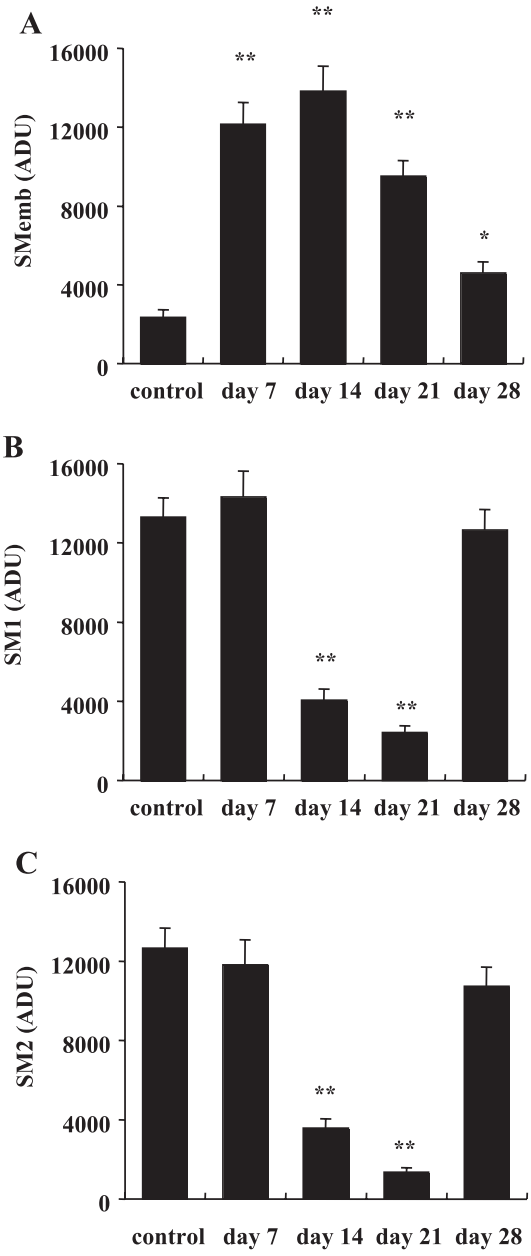

Fig. 8. Densitometric analysis of immunohistochemical staining with SMemb (*A*), SM1 (*B*), and SM2 (*C*) antibodies on each day. $*P < 0.05$ vs. control. $**P < 0.01$ vs. control. ADU, arbitrary densitometric units.

297.3 ± 44.4, and 220.5 ± 23.8 ($n = 4$), respectively. The collagen concentration on *day 14* was statistically higher than on the other days ($P < 0.05$), although the differences in collagen concentration between the control and SAH arteries on *days 7*, *21*, and *28* were not statistically significant. The data are shown in Fig. 9.

DISCUSSION

Changes in the Biomechanics of Vascular Smooth Muscle in Canine Basilar Arteries

The results of this study showed that the angiographic vasospasm in the two-hemorrhage canine model was severest on *days 7* and *14*. The angiographic diameter of the canine basilar artery gradually increased by *day 21*, and it had almost returned to the control level on *day 28*. The time course of experimental vasospasm in this model is similar to that in human patients (12, 35). We performed isometric tension studies on canine basilar arteries obtained at these points to investigate them for biomechanical changes.

Contrary to the results for angiographic vasospasm, the maximal contraction of the canine basilar arteries elicited with high-K^+ solution diminished until *day 21* and showed some recovery on *day 28*. In the study of measuring papaverine-sensitive and -insensitive tones, the papaverine-sensitive component was assumed to represent the myogenic component, and the papaverine-insensitive component was assumed to represent the nonmyogenic component. The papaverine-insensitive component was defined as the stiffness of the arterial wall. The study measuring papaverine-sensitive and -insensitive tone in canine basilar arteries revealed that myogenic tone decreased as vasospasm progressed on the angiograms. Although angiographic vasospasm showed significant recovery on *days 21* and *28*, nonmyogenic tone remained high until *day 28*. Because papaverine-insensitive, nonmyogenic tone is defined as "stiffness" of the artery, it can be concluded that the wall of vasospastic cerebral arteries undergoes significant changes in the stiffness as vasospasm progresses and that the stiffness does not recover despite improvement in the angiographic diameter of the canine basilar artery after SAH.

This evidence clearly demonstrates that the angiographic vasospasm after SAH in the late phase is not attributable to the active myogenic tone of vascular smooth muscle, but that it may be due to biomechanical changes in vascular smooth muscle. Because the great stiffness of arterial walls during cerebral vasospasm or even during the recovery period strongly suggested that histological changes occur in the arterial wall, we investigated the artery for histological changes associated with cerebral vasospasm.

Histological Findings in the Arterial Walls and the Collagen Concentrations of Arteries

Histological examination of hematoxylin-eosin-stained arteries revealed thickening of the medial smooth muscle layer on *days 7* and *14* and progression by *day 21*. Shortened and rounded configurations of smooth muscles cells were observed on *days 7*, *14*, and *21*, and the most prominent changes were

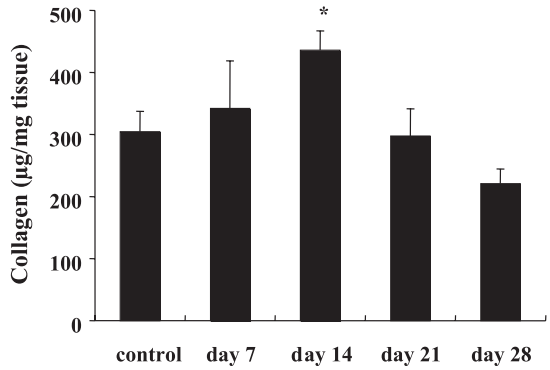

Fig. 9. Collagen concentration of canine basilar arteries on different days, measured by a quantitative dye-binding method designed for in vitro analysis of collagen. Data are expressed as μg/mg tissue and reported as means ± SE. $*P < 0.05$ vs. control, *days 7*, *14*, *21*, and *28*.

observed on *day 21*. Connective tissue visualized by Azan staining had increased in the medial layer on *day 7*, and the medial smooth muscle layer had consisted of much abundant connective tissue by *day 21*. These changes in both hematoxylin-eosin staining and Azan staining gradually returned to the appearance of the control on *day 28*. Although short, round smooth muscle cells were still observed on *day 28*, the medial thickening and amount of connective tissue in the medial layer had decreased. No clear changes in collagen levels were observed except on *day 14*. The above findings indicate that the increased connective tissue in the medial smooth muscle layer is not attributable to collagen and may be related to another protein.

Several markers of phenotypic changes and/or the differentiation status of smooth muscle have been described (1, 15, 16, 19), and the MHC of smooth muscle has been found to be the most specific molecular marker for detection of such changes (15, 16, 19). Immunohistochemical studies with monoclonal antibodies against SMemb, SM1, and SM2 showed very little SMemb immunoreactivity and the presence of abundant SM1 and SM2 reactivity in the control artery, indicating complete differentiation in the control canine basilar artery. SMemb immunoreactivity was observed on *day 7* and continued until *day 21*, and SM1 and SM2 immunoreactivities were no longer seen on *day 14* and *day 21*, indicating that the vasospastic canine basilar artery had undergone dedifferentiation. On *day 28*, SMemb immunoreactivity was much weaker, and SM1 and SM2 immunoreactivity was reobserved. Quantitative analysis of immunoreactivity against SMemb, SM1, and SM2 clearly indicated these changes. The histological findings in the hematoxylin-eosin-stained and Azan-stained specimens and the immunohistochemical findings with anti-SMemb, SM1, and SM2 antibodies were well correlated. The two parameters, the time course of appearance of synthetic-type smooth muscle cells, which has high potency of protein synthesis, and that of increased connective tissue in the arterial wall, are paralleled. Thus phenotypic changes in vascular smooth muscle occur in long-lasting vasospastic cerebral arteries.

Correlations Between the Biomechanical and Histological Change in Cerebral Arteries in the Mechanism of Cerebral Vasospasm After SAH

As shown by the measurement of maximal force generated in response to a high-K^+ solution, it is clear that prolonged cerebral vasospasm after SAH is not attributable to active myogenic tone. The results of our study examining the level of myogenic tone and stiffness of the arterial wall in canine basilar arteries also support this conclusion. In addition, as histological and immunohistochemical studies correlated with the time course of angiographic vasospasm, especially during prolonged cerebral vasospasm after *day 7*, the mechanism sustaining cerebral vasospasm after SAH is due to biomechanical changes, especially phenotypic changes of vascular smooth muscle, as well as histological changes. Dedifferentiated vascular smooth muscle synthesizes mesodermal matrix in the medial layer of the arterial wall and induces thickening of the arterial wall. This synthesis of mesodermal matrix is likely due not to collagen, but to some other protein. In a sense, these changes represent hypertrophic remodeling of the arterial wall (2, 5, 9) and could be an important mechanism of the cerebral vasospasm after *day 7*. The redifferentiation of the arterial wall was associated with recovery from cerebral vasospasm. Myogenic tone, however, did not return to control levels by *day 28* in our study. This result is surprising in view of the evidence of reexpression of SM1 and SM2 (contractile type of smooth muscle MHC) in the immunohistochemical studies. One explanation for this is that the redifferentiated new smooth muscle may have not recovered contractile capacity at this stage of the vasospasm, and further investigation is necessary to clarify the reason for the discrepancy.

In conclusion, the present study demonstrates that significant phenotypic changes occur in smooth muscle of major cerebral vasospastic arteries after SAH for longer than a week. During this period, cerebral vasospasm prolongs despite attenuation of myogenic contractility of the artery. Not only qualitative but also quantitative demonstrations of such evidence in the present experiment strongly suggest that the main role to sustain prolonged vasospasm might shift in the time course of cerebral vasospasm and the roles of arterial wall stiffness may play a pivotal role, especially in the prolonged vasospasm. In the viewpoint of the treatment of cerebral vasospasm, tactics for the treatment of vasospasm, which changes with time, should be considered on the basis of the pathophysiological mechanism.

REFERENCES

1. **Aikawa M, Sivam PN, Kuro-o M, Kimura K, Nakahara K, Takewaki S, Ueda M, Yamaguchi H, Yazaki Y, and Periasamy M.** Human smooth muscle myosin heavy chain isoforms as molecular markers for vascular development and atherosclerosis. *Circ Res* 73: 1000–1012, 1993.
2. **Baumbach GL and Ghoneim S.** Vascular remodeling in hypertension. *Scanning Microsc* 7: 137–143, 1993.
3. **Bevan JA, Bevan RD, and Frazee JG.** Functional arterial changes in chronic cerebrovasospasm in monkeys: an in vitro assessment of the contribution to arterial narrowing. *Stroke* 18: 472–481, 1987.
4. **Borel CO, McKee A, Parra A, Haglund MM, Solon A, Prabhakar V, Sheng H, Warner DS, and Niklason L.** Possible role for vascular cell proliferation in cerebral vasospasm after subarachnoid hemorrhage. *Stroke* 34: 427–433, 2003.
5. **Chrysant SG.** Vascular remodeling: the role of angiotensin-converting enzyme inhibitors. *Am Heart J* 135: S21–S30, 1998.
6. **Findaly JM, Weir BK, Kanamaru K, and Espinosa F.** Arterial wall changes in cerebral vasospasm. *Neurosurgery* 25: 736–746, 1989.
7. **Halayko AJ and Solway J.** Molecular mechanisms of phenotypic plasticity in smooth muscle cells. *J Appl Physiol* 90: 358–368, 2001.
8. **Hirst SJ, Walker TR, and Chilvers ER.** Phenotypic diversity and molecular mechanism of airway smooth muscle proliferation in asthma. *Eur Respir J* 16: 159–177, 2000.
9. **Intengan HD and Schiffrin EL.** Vascular remodeling in hypertension: roles of apoptosis, inflammation, and fibrosis. *Hypertension* 38: 581–587, 2001.
10. **Iwasa K, Bernanke DH, Smith RR, and Yamamoto Y.** Nonmuscle arterial constriction after subarachnoid hemorrhage: role of growth factors derived from platelets. *Neurosurgery* 32: 619–624, 1993.
11. **Jackowski A, Crockard A, Burnstock G, Russel RR, and Kristek F.** The time course of intracranial pathophysiological changes following experimental subarachnoid haemorrhage in the rat. *J Cereb Blood Flow Metab* 10: 835–849, 1990.
12. **Kapp JP, Neill WR, Neil CR, Hodges LR, and Smith RR.** The three phases of cerebral vasospasm. *Surg Neurol* 18: 40–45, 1982.
13. **Kim P, Sundt TM Jr, and Vanhoutte PM.** Alterations of mechanical properties in canine basilar arteries after subarachnoid hemorrhage. *J Neurosurg* 71: 430–436, 1989.
14. **Koide M, Nishizawa S, Ohta S, Yokoyama T, and Namba H.** Chronological changes of the contractile mechanism in prolonged vasospasm after subarachnoid hemorrhage: from protein kinase C to protein tyrosine kinase. *Neurosurgery* 51: 1468–1476, 2002.

15. **Kuro-o M, Nagai R, Tsuchimochi H, Katoh H, Yazaki Y, Ohkubo A, and Takaku F.** Developmentally regulated expression of vascular smooth muscle myosin heavy chain isoforms. *J Biol Chem* 264: 18272–8275, 1989.
16. **Kuro-o M, Nagai R, Nakahara K, Katoh H, Tsai RC, Tsuchimochi H, Yazaki Y, Ohkubo A, and Takaku F.** cDNA cloning of a myosin heavy chain isoform in embryonic smooth muscle and its expression during vascular development and in arteriosclerosis. *J Biol Chem* 266: 3768–3773, 1991.
17. **Lyons MA, Shukla R, Zhang K, Pyne GJ, Singh M, Biehle SJ, and Clark JF.** Increase of metabolic activity and disruption of normal contractile protein distribution by bilirubin oxidation products in vascular smooth-muscle cells. *J Neurosurg* 100: 505–511, 2004.
18. **Mayberg MR, Okada T, and Bark DH.** Morphological changes in cerebral arteries after subarachnoid hemorrhage. *Neurosurg Clin N Am* 1: 417–432, 1990.
19. **Nagai R, Kuro-o M, Babij P, and Periasamy M.** Identification of two types of smooth muscle heavy chain isoforms by cDNA cloning and immunoblot analysis. *J Biol Chem* 264: 9734–9737, 1989.
20. **Nakajima N, Nagahiro S, Sano T, Satomi J, and Satoh K.** Phenotypic modulation of smooth muscle cells in human cerebral aneurysmal walls. *Acta Neuropathol (Berl)* 100: 475–480, 2000.
21. **Nakayama K.** Active, and passive mechanical properties of ring and spiral segments of isolated dog basilar artery assessed by electrical and pharmacological stimulations. *Blood Vessels* 25: 285–298, 1988.
22. **Nishizawa S, Nezu N, and Uemura K.** Direct evidence for a key role of protein kinase C in the development of vasospasm after subarachnoid hemorrhage. *J Neurosurg* 76: 635–639, 1992.
23. **Nishizawa S, Peterson JW, Shimoyama I, and Uemura K.** Relation between protein kinase C and calmodulin systems in cerebrovascular contraction: investigation of the pathogenesis of vasospasm after subarachnoid hemorrhage. *Neurosurgery* 31: 711–716, 1992.
24. **Nishizawa S, Yamamoto S, and Uemura K.** Interrelation between protein kinase C and nitric oxide in the development of vasospasm after subarachnoid hemorrhage. *Neurol Res* 18: 89–95, 1996.
25. **Nishizawa S, Obara K, Nakayama K, Koide M, Yokota N, and Ohta S.** Protein kinase Cδ and α are involved in the development of vasospasm after subarachnoid hemorrhage. *Eur J Pharmacol* 398: 113–119, 2000.
26. **Nishizawa S, Obara K, Koide M, Nakayama K, Ohta S, and Yokoyama T.** Attenuation of canine cerebral vasospasm after subarachnoid hemorrhage by protein kinase C inhibitors despite augmented phosphorylation of myosin light chain. *J Vasc Res* 40: 168–179, 2003.
27. **Owens GK.** Regulation of differentiation of vascular smooth muscle cells. *Physiol Rev* 75: 487–517, 1995.
28. **Pluta RM, Zauner A, Morgan JK, Muraszko KM, and Oldfield EH.** Is vasospasm related to proliferative arteriopathy? *J Neurosurg* 77: 740–748, 1992.
29. **Ross R.** The pathogenesis of atherosclerosis: a perspective for the 1990s. *Nature* 362: 801–809, 1993.
30. **Sasaki S, Ohue S, Kohno K, and Takeda S.** Impairment of vascular reactivity and changes in intracellular calcium levels of smooth muscle cells in canine basilar arteries after subarachnoid hemorrhage. *Neurosurgery* 25: 753–761, 1989.
31. **Schwartz SM, Campbell GR, and Campbell JH.** Replication of smooth muscle cells in vascular disease. *Circ Res* 58: 427–444, 1986.
32. **Smith RR, Clower BR, Grotendorst GM, Yabuno N, and Cruse JM.** Arterial wall changes in early human vasospasm. *Neurosurgery* 16: 171–176, 1985.
33. **Smith RR, Clower BR, Cruse JM, Honma Y, and Haining JL.** Constrictive structural elements in human cerebral arteries following aneurysmal subarachnoid haemorrhage. *Neurol Res* 9: 188–192, 1987.
34. **Varsos VG, Liszczak TM, Han DH, Kistler JP, Vielma J, Black PM, Heros RC, and Zervas NT.** Delayed cerebral vasospasm is not reversible by aminophylline, nifedipine, or papaverine in a "two-hemorrhage" canine model. *J Neurosurg* 58: 11–17, 1983.
35. **Weir B, Grace M, Hansen J, and Rothberg C.** Time course of vasospasm in man. *J Neurosurg* 48: 173–178, 1978.
36. **Zubkov AY, Tibbs RE, Clower B, Ogihara K, Aoki K, and Zhang JH.** Morphological changes of cerebral arteries in a canine double hemorrhage model. *Neurosci Lett* 326: 137–141, 2002.